International Journal of Pharmaceutics 654 (2024) 123946

Contents lists available at ScienceDirect

International Journal of Pharmaceutics

journal homepage: www.elsevier.com/locate/ijpharm

# High loading of lipophilic compounds in mesoporous silica for improved solubility and dissolution performance

Marvin Benedikt Brenner [a], Matthias Wüst [b], Martin Kuentz [c], Karl G. Wagner [a,*]

[a] University of Bonn, Pharmaceutical Institute, Department of Pharmaceutics, Gerhard-Domagk-Str. 3, 53121 Bonn, Germany
[b] University of Bonn, Institute of Nutritional and Food Sciences, Food Chemistry, Friedrich-Hirzebruch-Allee 7, 53115 Bonn, Germany
[c] University of Applied Sciences and Arts Northwestern Switzerland, Institute of Pharma Technology, Hofackerstr. 30, 4132 Muttenz, Switzerland

ARTICLE INFO

*Keywords:*
Bioavailability improvement
Dissolution
Drug loading
Extracts
Mesoporous silica
Solubility enhancement

ABSTRACT

Loading poorly soluble active pharmaceutical ingredients (API) into mesoporous silica can enable API stabilization in non-crystalline form, which leads to improved dissolution. This is particularly beneficial for highly lipophilic APIs (log $D_{7.4} > 8$) as these drugs often exhibit limited solubility in dispersion forming carrier polymers, resulting in low drug load and reduced solid state stability. To overcome this challenge, we loaded the highly lipophilic natural products coenzyme Q10 (CoQ10) and astaxanthin (ASX), as well as the synthetic APIs probucol (PB) and lumefantrine (LU) into the mesoporous silica carriers Syloid® XDP 3050 and Silsol® 6035. All formulations were physically stable in their non-crystalline form and drug loads of up to 50 % were achieved. At increasing drug loads, a marked increase in equilibrium solubility of the active ingredients in biorelevant medium was detected, leading to improved performance during biorelevant biphasic dissolution studies (BiPHa + ). Particularly the natural products CoQ10 and ASX showed substantial benefits from being loaded into mesoporous carrier particles and clearly outperformed currently available commercial formulations. Performance differences between the model compounds could be explained by *in silico* calculations of the mixing enthalpy for drug and silica in combination with an experimental chromatographic method to estimate molecular interactions.

## 1. Introduction

To achieve sufficient bioavailability, it is necessary to first dissolve an adequate dose fraction of the active pharmaceutical ingredient (API) in an aqueous gastrointestinal fluid (Barthe et al., 1999; Martinez and Amidon, 2002). High API concentrations in solution increase the driving force for absorption through the intestinal membrane (Taylor and Zhang, 2016). Subsequent to the absorption, the API enters systemic circulation and is transported to the relevant side of action where the biological activity can take place (Martinez and Amidon, 2002). Unfortunately, a decrease in water solubility limits the dissolution, absorption and hence bioavailability of active ingredients, whereby a high degree of compound lipophilicity and/or hydrophobicity are key factors (Ditzinger et al., 2019a). Compounds that have high Tm values and low to moderate log P values are commonly referred to as 'brick-dust' compounds, whereas those with low Tm values and high log P values are known as 'grease balls'. The brick-dust compounds have limited solubility by their solid-state, where the breakdown of the crystal lattice is the most challenging step. On the other hand, the grease balls have the solvation step in water as the primary obstacle for drug dissolution (Ditzinger et al., 2019a). This becomes particularly problematic considering that roughly 40–90 % of the APIs currently in development encounter solubility issues (Loftsson and Brewster, 2010; Ting et al., 2018). However, this problem is not only limited to synthetic APIs but also affects substances of natural origin. Especially tri- and tetraterpenes (e.g. astaxanthin and coenzyme Q10) experience reduced water solubility, attributed to their lipophilic isoprenoid chains (Atriya et al., 2023; Schulz et al., 2006). Absorption via the lymphatic pathway after incorporation into chylomicrons can be assumed to occur for this type of lipophilic natural products (Schulz et al., 2006). Nevertheless, the lymphatic pathway also requires *in situ* micellization of the dissolved API with the aid of bile salts and absorption only occurs after emulsification

*Abbreviations:* ACN, acetonitrile; ASD, amorphous solid dispersion; ASX, astaxanthin; Bi - FaSSIF - V2, biphasic dissolution adapted intestinal fluid V2; CoQ10, coenzyme Q10; DAD, diode array detector; DCM, dichloromethane; FID, flame ionization detector; HS, head space; LU, lumefantrine; PB, probucol; Rf, retarding front; TLC, thin layer chromatography.

* Corresponding author at: University of Bonn, Pharmaceutical Institute, Department of Pharmaceutics, Gerhard-Domagk-Str. 3, 53121 Bonn, Germany.
*E-mail address:* karl.wagner@uni-bonn.de (K.G. Wagner).

https://doi.org/10.1016/j.ijpharm.2024.123946
Received 25 January 2024; Received in revised form 22 February 2024; Accepted 22 February 2024
Available online 27 February 2024

(Managuli et al., 2018). Addressing this concern, several approaches have been suggested to improve absorption of highly lipophilic APIs, which includes lipid-based formulations targeting enhanced solubilization and an increase in absorption through the lymphatic pathway (Schulz et al., 2006). The surfactants and lipids contained in especially the self-emulsifying formulations promote integration of the API in micellar inclusion complexes even when only small solvent volumes are present (Neslihan Gursoy and Benita, 2004). However, the bioavailability improvement achieved by these formulations may sometimes be compromised, as the formation of stable micellar complexes can hinder intestinal absorption accompanied by the overall issue of limited dose strength of lipid-based systems.

One of the most preferred techniques, that is widely used for increasing solubility and bioavailability especially of poorly soluble synthetic APIs, is stabilizing the drug in its amorphous state. Amorphous materials have higher solubility and dissolve faster than their crystalline counterparts (Taylor and Zhang, 2016). Unlike the crystalline form, dissolving amorphous material does not require breaking of the crystal lattice structure so concentrations can be reached beyond the thermodynamic solubility (Singh and Van den Mooter, 2016). Consequently, various strategies have been postulated to hinder recrystallization while maintaining the solubility benefits of an amorphous molecular structure (Brouwers et al., 2009). These approaches include co-grinding (Li et al., 2019a), co-amorphous formulations (Karagianni et al., 2018), preparation of polymer-based amorphous solid dispersions (ASD) (Baghel et al., 2016; Pöstges et al., 2022; Taylor and Zhang, 2016), or mesoporous silica-based systems (Hate et al., 2020; McCarthy et al., 2018; Price et al., 2019; Vraníková et al., 2020). Considering ASDs, polymeric excipients decrease molecular mobility of the API and thereby enable a stabilization in amorphous form, although this is thermodynamically unfavorable (Bookwala and Wildfong, 2023). Nonetheless, this strategy can pose a challenge for lipophilic active ingredients, as poor solubility in the polymer matrix results in limited drug loading and eventually formulation instability as high kinetic concentrations in the polymer matrix elevate the risk of recrystallization and phase separation during storage (Janssens and Van den Mooter, 2009; Wolbert et al., 2022).

Another proven technique for maintaining active ingredients in a non-crystalline form is using mesoporous silica particles as a carrier material (Ditzinger et al., 2019b; Niederquell et al., 2023). Drug loading can be achieved either with solvent-based techniques, for example incipient wetness impregnation or by solvent-free methods like drug melting or the use of supercritical fluids (Li et al., 2019b; Seljak et al., 2020). Mesoporous systems are known for their ability to inhibit the crystallization process of drugs by confining them in carrier pores, especially if the pore size is comparable to the critical nuclei size. Shen et al. (2017) suggested that a drug would remain in a non-crystalline form within the mesopores if the pore size were smaller than 12 times the molecular size of the API (Shen et al., 2017). More refined estimates can be found in the literature based on the classical theory of homogeneous nucleation assuming that only nuclei larger than a critical nucleation size can grow and cause formulation instability (Descamps and Willart, 2018; Knapik et al., 2016; Vraníková et al., 2020). Furthermore, the molecular mobility of APIs incorporated in small enough pores is significantly lower than in the bulk (Vraníková et al., 2020). Consequently, there is not surrounding polymer matrix needed as in case of ASDs, which appears beneficial for enabling the use of highly lipophilic/ poorly soluble APIs. Comparable to ASDs, the non-crystalline form allows for a significantly higher release of active ingredients than the crystalline molecular form. In addition, Le et al. (2019) observed an increase in dissolution performance as drug load increased, even surpassing the theoretical monolayer capacity of Syloid® XDP 3050 used as a carrier (Le et al., 2019). Dening and Taylor, on the other hand, observed a notable decrease in diffusive flux for ritonavir loaded SBA-15 when the theoretical monolayer surface coverage was exceeded (Dening and Taylor, 2018). Accordingly, the effects of different drug loads on solubility and release of different APIs from mesoporous silica carriers has not yet been fully elucidated und further work is necessary.

The aim of our study was to explore how various drug loads of highly lipophilic (log $D_{7.4} > 8$) synthetic APIs (probucol and lumefantrine) and natural products (coenzyme Q10 and astaxanthin) impact the solubility and dissolution behavior of the active ingredients in various media. The term natural product refers to extracts of natural origin, which are composed of several structurally related but not identical active ingredients. The astaxanthin enriched oleoresin contains more than 20 different mono- and diesters of astaxanthin. Thereby the sum of all individual components is referred to as “the active ingredient”. By comparison, synthetic APIs typically consist of only one molecular species with precisely known structural identity. Syloid® XDP 3050 (average pore diameter: 22.9 nm (Waters et al., 2018)) and Silsol® 6035 (average pore diameter: 6.0 nm (Cokenakes, 2021)) were used as mesoporous carriers. In addition, the suitability of this formulation principle for improving the biorelevant dissolution performance of the highly lipophilic and poorly soluble model APIs was investigated using a biphasic dissolution assay.

## 2. Materials and methods

### 2.1. Materials

Coenzyme Q10 (CoQ10) (purity ≥ 99.1 %, CAS 303–98-0) from Abcr GmbH (Karlsruhe, Germany), astaxanthin (ASX) enriched *Haematococcus pluvialis* oleoresin (10.1 % ASX content) from BDI-BioLife Science GmbH (Hartberg, Austria), probucol (PB) (purity ≥ 99.7 %, CAS 23288–49-5) and lumefantrine (LU) (purity ≥ 99.6 %, CAS 82186–77-4), both from Swapnroop Drugs & Pharmaceuticals (Aurangabad, India), were used as model compounds. CoQ10 oily dispersion (Nature Made® $CoQ_{10}$, Pharmavite®, Northridge, CA, USA), CoQ10 micelles (NovaSOL® Q, Aquanova AG, Darmstadt, Germany) and astaxanthin micelles (NovaSOL® Astaxanthin, Aquanova AG, Darmstadt, Germany) were used as reference market formulations. Syloid® XDP 3050 (average pore diameter: 22.9 nm, pore volume 1.69 $cm^3/g$, surface area 287 $m^2/g$ (Waters et al., 2018)) and Silsol® 6035 (average pore diameter: 6.0 nm, pore volume 0.90 $cm^3/g$, surface area 476 $m^2/g$ (Cokenakes, 2021)) were donated by Grace GmbH (Worms, Germany). Tri-potassium phosphate, sodium hydroxide (VWR Chemicals, Darmstadt, Germany) and tri-potassium citrate (Carl Roth, Karlsruhe, Germany) were used as buffer concentrate. Sodium dihydrogen phosphate and di-sodium hydrogen phosphate (VWR Chemicals, Darmstadt, Germany) were used to generate 0.1 M phosphate buffer (pH 6.8). Sodium taurocholate, lecithin, 0.1 N hydrochloric acid (HCl) and 1-decanol were obtained from VWR Chemicals (Darmstadt, Germany). Formic acid, dimethyl sulfoxide (DMSO) and HPLC grade solvents ethanol, methanol, acetone, dichloromethane (DCM) and acetonitrile (ACN) were purchased from VWR Chemicals (Fontenay-sous-Bois, France). HPLC grade water was received from Fisher Chemicals (Loughborough, UK).

### 2.2. Preparation of drug loaded mesoporous silica particles

Mesoporous silica was loaded using incipient wetness impregnation (Trzeciak et al., 2021). Different concentrations of CoQ10, ASX, PB and LU in DCM were used. For evaluation of drug-load-dependent solubility in biorelevant medium, silica with drug loads between 0.1 % and 50 % (*w/w*) (refer to **Table S1** and Fig. 4) were produced. Solubility of the compounds in DCM limited the maximum achievable drug load to the values as shown in Table 1. Due to different pore volumes, 1.50 mL/g of DCM was used for loading of XDP 3050 and 0.75 mL/g for Silsol 6035. Under continuous stirring, the DCM stock solutions (SL) were added stepwise to the silica powder in a beaker. Stirring was continued until all the liquid was absorbed into the pores and a seemingly dry powder was obtained. Subsequently, the formulations were protected from light and the solvent was evaporated under atmospheric conditions for 24 h in a drying oven. Residual solvent analysis was performed by headspace (HS)

**Table 1**
Preparation of loaded mesoporous silica; including the maximum achievable drug concentration in the dichloromethane (DCM) stock solution (applied solvent volume for drug loading: 1.50 mL/g (XDP 3050) and 0.75 mL/g (Silsol 6035)) and the total drug load (*w/w*) of the obtained formulation (determined by HPLC).[a]

| Formulation | Concentration in DCM stock solution [mg/mL] | Total Drug Load [%] |
|---|---|---|
| CoQ10: Silsol 6035 | 670 | 33.1 |
| CoQ10: XDP 3050 | 670 | 49.8 |
| ASX: Silsol 6035[a] | 67 | 3.3 |
| ASX: XDP 3050[a] | 67 | 5.9 |
| PB: Silsol 6035 | 290 | 17.8 |
| PB: XDP 3050 | 290 | 30.3 |
| LU: Silsol 6035 | 290 | 17.9 |
| LU: XDP 3050 | 290 | 30.1 |

[a] ASX content of *Haematococcus pluvialis* oleoresin used for silica loading was 10.1%, therefore the total drug load was reduced.

– gas chromatography (GC) (refer to 2.4; GC detection of residual solvent). Drug load was evaluated by high performance liquid chromatography (HPLC) (refer to 2.3; HPLC method).

### 2.3. HPLC method

CoQ10, ASX, PB and LU were quantified using a Shimadzu HPLC system (LC-2010A HT, Shimadzu Corporation, Kyoto, Japan). Four different HPLC methods were used (Table 2) (Miao et al., 2006; Mosca et al., 2002). A Nucleodur C18ec column (250 mm x 4.6 mm, 3 µm particle size, Macherey-Nagel, Düren, Germany) was used for samples containing CoQ10 and ASX and a LiChrospher RP-18 column (125 mm x 4.6 mm, 5 µm particle size, Merck Millipore, Billerica, MA, USA) was used for PB and LU quantification. The column temperature was set to 40.0 °C and LabSolutions software (Shimadzu Corporation, Kyoto, Japan) was used for monitoring and integration of all peaks. For drug load quantification of mesoporous silica formulations, samples equivalent to 10 mg active ingredient were sonicated for 10 min with 50.0 mL DCM in an amber colored volumetric flask. Subsequently, samples were collected, immediately filtered through a 0.22 µm poly(tetrafluoroethylene) (PTFE) syringe filter and 10 µL (1 µL for ASX containing samples) were directly injected into the HPLC system. Sample collection was also performed for determination of apparent and equilibrium solubility and after each dissolution run. Standard curves were prepared freshly for each run and served as reference for quantification and for correct peak identification.

### 2.4. Gas chromatographic (GC) detection of residual solvent

Residual content of DCM after drying was analyzed using a Focus GC connected to a TriPlus RSH Autosampler unit (Thermo Fischer Scientific, Waltham, MA, USA). A FS_CS_624 capillary column (30 m x 0.32 mm, 1.8 µm film thickness, 6 % cyanopropylpolysiloxane, CS-Chromatographie Service GmbH, Langerwehe, Germany) was used for all measurements. Analysis was performed in headspace (HS) modus and a flame ionization detector (FID) set to 240 °C was used for detection. Accurately weighed samples of 50 mg were mixed with 1.0 mL DMSO and incubated at 50 °C for 10 min. Subsequently, 1.0 mL of the gas phase was injected into the GC and the column oven was heated from 50 to 140 °C at a rate of 10 °C/min, followed by a 4 min plateau at 140 °C. Nitrogen (2.0 mL/min) was used as carrier gas and a split flow of 1/5 was applied during injection.

**Table 2**
Composition of the mobile phases (*v/v*), solvent flow and detection wavelength used for coenzyme Q10, astaxanthin, probucol and lumefantrine quantification.

| Active ingredient | Mobile phase A | Mobile phase B | Flow [mL/min] | Elution | Detection wavelength [nm] |
|---|---|---|---|---|---|
| Coenzyme Q10 | ethanol (65 %) | methanol (35 %) | 1.00 | isocratic | 275 |
| Astaxanthin | acetone (83–98 %) | water (17–2 %) | 0.80 | gradient (60 min) | 474 |
| Probucol | ACN (90 %) | water (10 %) | 1.00 | isocratic | 254 |
| Lumefantrine | ACN (90 %) | water (10 %) | 1.00 | isocratic | 350 |

### 2.5. X-ray powder diffraction (XRPD)

X-ray Powder Diffraction (XRPD) was conducted in reflection mode using an ẊPert MRD Pro (PAN-alytical, Alemlo, The Netherlands) at 45 kV and 40 mA with an ẊCelerator detector and nickel filtered CuKα1 radiation. Scanning range was set from 5 to 45° 2θ with a step size of 0.017° 2θ.

### 2.6. Differential Scanning Calorimetry (DSC)

Differential Scanning Calorimetry (DSC) measurements were performed by utilizing a Mettler-Toledo DSC 2 (Gießen, Germany) equipped with a nitrogen cooling system and nitrogen as purge gas (30 mL/min). Samples of approximately 10 mg were accurately weighed into aluminum pans with a pierced lid. A conventional method, consisting of a heating cycle from 25 to 100 °C (CoQ10 and ASX) or to 170 °C (PB and LU) with a constant heat rate of 10 °C/min was used for all measurements.

### 2.7. Equilibrium solubility

For determination of equilibrium solubility in various media (0.1 N HCl, phosphate buffer pH 6.8, Bi-FaSSIF-V2 pH 6.8 and 1-decanol) the shake flask method was used (Table 3). Sodium taurocholate and lecithin were added to 0.1 M phosphate buffer (pH 6.8) to generate biphasic dissolution adapted-fasted state simulated intestinal Fluid-V2 (Bi-

**Table 3**
Molecular weight (MW), $pK_a$ values (Mano et al., 2018; Patel et al., 2013; Probucol: DrugBank Online; Trumpower, 2012), log $D_{7.4}$ (du Plessis et al., 2015; Gershkovich and Hoffman, 2005; Jannel et al., 2020; Sy et al., 2012), number of H-bond donors and acceptors (predicted by ChemAxon), and saturation solubility in 0.1 N HCl, phosphate buffer pH 6.8, Bi-FaSSIF-V2 and 1-decanol (determined by HPLC) of coenzyme Q10, astaxanthin, probucol and lumefantrine (mean ± SD); n = 3.

| Parameter | Coenzyme Q10 | Astaxanthin[a] | Probucol | Lumefantrine |
|---|---|---|---|---|
| **MW [g/mol]** | 863.3 | 596.8 | 516.8 | 528.9 |
| **published log $D_{7.4}$** | 14.7 | 13.3 | 10.9 | 8.3 |
| **published $pK_a$** | 13.3 | 10.6 | 10.3 | 8.2 |
| **Number of H-bond donors** | 0 | 2 | 2 | 1 |
| **Number of H-bond acceptors** | 4 | 4 | 2 | 2 |
| **S (0.1 N HCl) [µg/mL]** | 0.1 ± 0.0 | 0.3 ± 0.1 | 3.3 ± 0.4 | 1.5 ± 0.2 |
| **S (Buffer pH 6.8) [µg/mL]** | 0.1 ± 0.0 | 0.4 ± 0.2 | 0.9 ± 0.3 | 0.2 ± 0.1 |
| **S (Bi-FaSSIF-V2) [µg/mL]** | 5.5 ± 2.3 | 1.1 ± 1.4 | 2.0 ± 1.2 | 2.1 ± 0.1 |
| **S (1-decanol) [µg/mL]** | > 5000 | > 5000 | > 5000 | > 5000 |

[a] (with exception of the solubilities, all astaxanthin values are given for the unesterified molecule).

FaSSIF-V2) (Denninger et al., 2020). An excess of neat CoQ10, ASX, PB, and LU and their corresponding loaded silica formulations was incubated in 20.0 mL medium (aqueous/organic). The excess was at least 20 times the equilibrium solubility of each drug. With an increase in drug load of the silica formulations, the excess amount of active ingredient also increased. Experiments were performed using a GFL 1083 shaking incubator (Gesellschaft für Labortechnik GmbH, Burgwedel, Germany) at 37.0 °C ± 0.5 °C. After 48 h, samples of 1000 µL were collected, filtered through a 0.22 µm PTFE syringe filter and directly injected into the HPLC system (refer to 2.3 HPLC method).

### 2.8. Apparent solubility/ kinetic concentration

To determine the apparent solubility (i.e., kinetic concentrations) of CoQ10, ASX, PB and LU in biorelevant medium, solvent shift experiments were conducted. The same dissolution apparatus as for biphasic dissolution measurements was used (refer to section 2.11). In contrast to BiPHa + measurements the organic phase was omitted. Acetone stock solutions (SL) of CoQ10, ASX, PB and LU with concentrations of 40 mg/mL were prepared and the assays were initiated by adding 250 µL into 50.0 mL biorelevant medium to receive a potential concentration of 0.2 mg/mL. Concentrations were determined for 270 min (equivalent to biphasic dissolution) using an 8454 UV/VIS DAD spectrophotometer (Agilent, Waldbronn, Germany) including scattering correction (method). In addition, after 15 min and 270 min samples were collected, filtered and directly injected into the HPLC system.

### 2.9. Compound-silica interactions and in vitro drug release

#### 2.9.1. COSMO-RS calculations

To access the interactions between the amorphous silica surface of XDP 3050 and Silsol 6035 and the model drugs, simplified drug-silica bulk calculations were based on the software COSMO*quick* (BIOVIA COSMO*quick*, Version 2020, Dassault systems, France). The excess enthalpy ($H_{ex}$) of drug and silica was estimated at 37 °C as a measure of molecular drug-excipient interactions similar to Price et al (Price et al., 2019). $H_{ex}$ is also referred to as the enthalpy of mixing $\Delta H_{mix}$ with the advantage that the "self-cohesion" of the pure components is taken into account, compared to other interaction energy values, for example from molecular docking:

$$\Delta H_{mix} = \sum_k x_k H^k_{mix} - \sum_k x_k H^k_{pure} \quad (1)$$

In this general equation $x_k$ holds for the molar fraction of a component $k$, $H^k_{\mathrm{mix}}$ is the enthalpy of compound $k$ in the mixture, whereas $H^k_{pure}$ represents the enthalpy of the pure component $k$.

The use of $\Delta H_{mix}$ as interaction parameter is a simplification as it does not take the situation on the surface with the water phase into account. However, this binary drug-excipient interaction can exhibit rank-order performance correlations as it was, for example, reported in drug interactions with precipitation inhibitors (Price et al., 2019). For a more detailed description of the calculations performed within the software package, the reader is referred to (Loschen and Klamt, 2012).

#### 2.9.2. Thin layer chromatography (TLC)

In addition, thin layer chromatographic (TLC) experiments were carried out. Silica gel TLC plates with fluorescence indicator (silica gel 60 $F_{254}$, 10 cm x 10 cm) manufactured by Merck (Darmstadt, Germany) were used for the analysis. CoQ10, ASX, PB and LU were dissolved in DCM (1 mg/mL) and 2 µL of the optioned solutions were applied to the TLC plate, allowed to dry, and then eluted with petroleum ether - ethyl acetate - acetic acid 70:20:10 (*v/v/v*). Organic solvents were necessary to achieve sufficient eluting power. After evaporation of the eluent, the separated spots were visualized and marked under UV illumination at 254 nm and retarding- front (Rf) values were calculated.

#### 2.9.3. Monophasic non-sink dissolution

To ensure consistent hydrodynamics, the BiPHa + apparatus (refer to section 2.10) was used for the monophasic non-sink dissolution studies. Similar to the apparent solubility measurements, the organic phase was omitted. Loaded XDP 3050 or Silsol 6035 formulations (maximum drug load) equivalent to 10 mg of active ingredient were transferred to hard gelatine capsules (size 4) and introduced into the dissolution medium using a metal sinker. Concentrations were determined for 270 min (equivalent to biphasic dissolution) using an 8454 UV/VIS DAD spectrophotometer (Agilent, Waldbronn, Germany). In addition, the endpoint concentrations (270 min) were determined by HPLC.

### 2.10. Biorelevant biphasic dissolution

Biphasic dissolution studies were performed using a fully automated small scale dissolution device developed by Denninger et al. (2020) (Denninger et al., 2020). The device consisted of a water bath containing four cylindrical vessels (three samples and one blank) tempered to 37.0 ± 0.5 °C. Dissolution studies were performed with 50.0 mL of 0.1 N HCl (pH 1.0) as start medium to mimic the stomach conditions. After 30 min, the pH was increased stepwise from 1.0 to 5.5 (simulating the upper small intestine) and finally to 6.8 (simulating the lower small intestine) by adding McIlvaine buffer concentrate. Simultaneously Bi-FaSSIF-V2 (Denninger et al., 2020) was added to generate a biorelevant dissolution medium and the aqueous phase was covered with 50.0 mL of 1-decanol to simulate intestinal absorption. The endpoint of the dissolution measurements was set to 270 min. Samples equivalent to 10 mg CoQ10, ASX, PB or LU were accurately weighed into hard gelatine capsules (size 4) and introduced into the dissolution medium by a metal sinker with a mesh size of 1 mm. To prevent fine particulate and hydrophobic neat CoQ10, PB and LU from directly floating into the 1-decanol layer, dicalcium-phosphate tablets with 20 % drug load (equivalent to 10 mg active ingredient) were produced, grinded down using mortar and pestle and transferred to hard gelatine capsules. An Agilent 8454 UV/VIS DAD spectrophotometer (Agilent, Waldbronn, Germany) equipped with 1.0 mm flow-through cuvettes was used for concentration measurements in both media. Full flow filters with 1 µm pore size were used to reduce scattering in the aqueous medium caused by undissolved material. Remaining scattering during UV-measurements was eliminated using a LabView® application programmed by Denninger et al (Denninger et al., 2020). In addition, the endpoint concentrations (270 min) in both media were determined by HPLC (refer to Section 2.3).

## 3. Results

### 3.1. Physicochemical characterization

The molecular weight (MW) of the model compounds ranged from 516.8 to 863.3 g/mol, whereby the molar mass of naturally occurring ASX could increase to up to 1200 g/mol due to ester formation with fatty acids (Table 3). Corresponding to the molecular structures.

(Fig. 1), the log $D_{7.4}$ values were very high, ranging from 8.3 to 14.7. Attributed to the long isoprenoid chains, the natural products CoQ10 and ASX showed slightly higher log $D_{7.4}$ values in contrast to the synthetic APIs PB and LU. The $pK_a$ value were observed to be between 8.2 and 13.3 and while this was not physiologically relevant for an acidic $pK_a$, the basic nitrogen atom of LU was expected to be protonated along the gastrointestinal pH (basic $pK_a$ 8.2), introducing a charge into the molecule thereby increasing solubility. Accordingly, a 7.5 times higher solubility at pH 1 than at pH 6.8 was detected. For CoQ10 and ASX no pH dependent solubility behavior was observed. Nevertheless, for all tested compounds, low concentrations between 0.1 and 3.3 µg/mL were detected in aqueous media. However, when biorelevant surfactants like lecithin and taurocholate were added, solubility generally increased. CoQ10 showed the most significant improvement, with a 55-fold increase. However, only low absolute concentrations of the active

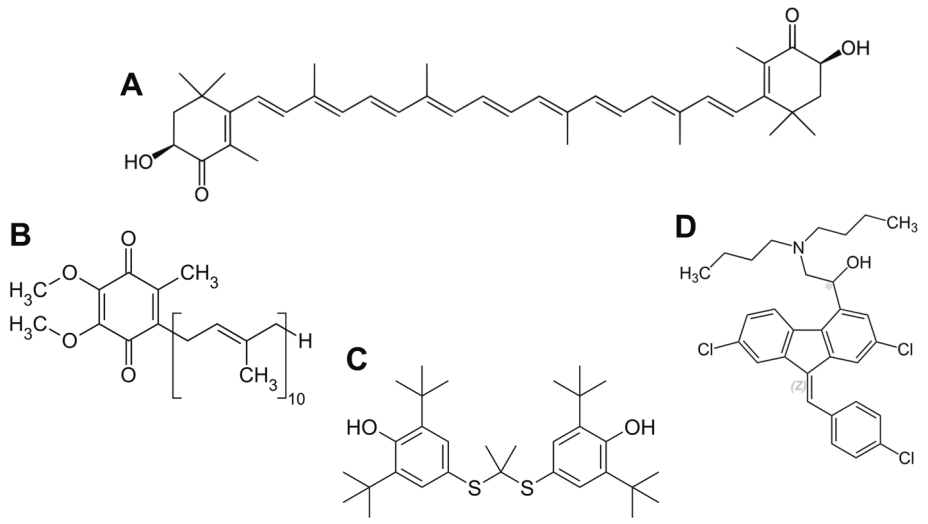


**Fig. 1.** Chemical structures of the model compounds: astaxanthin (A) (shown as unesterified molecule; the *Haematococcus pluvialis* extract contains manly mono- and diesters), coenzyme Q10 (B), probucol (C) and lumefantrine (D).

ingredients were observed ranging from 1.1 to 5.5 μg/mL in the medium even with surfactant addition. As a result, all media provided solubility-limited non-sink dissolution conditions. In contrast, model compounds exhibited solubility above 5 mg/mL in 1-decanol, indicating sink conditions in the absorption compartment during biorelevant biphasic dissolution studies.

### 3.2. GC detection of residual solvent

Incipient wetness impregnation was used for drug loading of the mesoporous silica. DCM was found to have the highest solution capability for the model compounds thereby enabling the highest possible drug load. Related to the toxicological side effects, DCM has a limit value of 600 ppm in oral pharmaceutical formulations (ICH Q3C (International council for harmonisation, 2021)). Thus, residual solvent detection using HS-GC-FID was performed (Table 4). Except for the PB-Silsol 6035 formulation (99.2 ± 15.3 ppm DCM) residual solvent amounts below 10 ppm were detected. The recovery of the method was tested at three concentration levels (40, 200 and 600 ppm) and was found to be 105.6 ± 1.7 %. Accordingly, the obtained results complied with the ICH guideline.

### 3.3. Solid state characterization

The solid state of the drug loaded silica formulations was investigated after manufacturing and drying using DSC (Fig. 2) and XRPD (Fig. 3). For simplicity, only the results for the formulations with the highest possible drug load were shown.

During the DSC experiments, it was observed that all highly loaded silica formulations lacked crystallinity, while the neat model compounds (excluding the ASX enriched oleoresin) had a crystalline structure. Neither the pure mesoporous silica nor the loaded silica formulations exhibited any glass transitions. Neat CoQ10, PB and LU, on the other hand, displayed sharp melting peak at 50.1 ± 0.8 °C, 127.2 ± 1.0 °C and 126.9 ± 1.3 °C, respectively. The ASX enriched oleoresin however contained ASX dissolved in a lipid-containing, semi-solid matrix, for which no melting peak was detected.

The DSC results were confirmed by XRPD measurements (Fig. 3). Regardless of the silica or lipophilic model compound examined, neither the pure mesoporous silica nor highly loaded formulations exhibited any detectable crystallinity. However, pure CoQ10 showed crystallinity, with distinct reflection peaks at 18.7° and 22.9° 2θ ASX displayed no remaining crystallinity due to the lipid-containing extract matrix, as mentioned above. In their unformulated state, both PB and LU exhibited sharp reflection peaks similar to CoQ10. For PB the highest intensity peaks were observed at 16.0°, 18.0°, and 19.1° 2θ, while for LU the peaks were observed at 5.6°, 21.0°, and 23.1° 2θ.

**Table 4**
Residual dichloromethane (determined by HS-GC-FID) in coenzyme q10, astaxanthin, probucol and lumefantrine loaded xdp 3050 and silsol 6035 formulations; $n = 6$.

| Active ingredient | Residual dichloromethane [ppm] | |
|---|---|---|
| | Silsol 6035 | XDP 3050 |
| **Coenzyme Q10** | < 10 | < 10 |
| **Astaxanthin** | < 10 | < 10 |
| **Probucol** | 99.2 ± 15.3 | < 10 |
| **Lumefantrine** | < 10 | < 10 |

### 3.4. Drug loading degree dependent solubility in biorelevant medium

The drug loading degree dependent solubility of all four model compounds was investigated in phosphate buffer pH 6.8 and biorelevant medium (Bi-FaSSIF-V2). In phosphate buffer the model compound concentrations measured were found to be only slightly increased when compared to the equilibrium solubility of the pure active ingredients (**Table S1** and **Table S2**). Contrastingly, in surfactant containing biorelevant medium the concentrations were strongly dependent on the loading degree of the mesoporous silica, except for a compound dependent loading quantity that had no effect on solubility (Fig. 4). In general, solubility was observed to increase linearly with the drug loading degree. However, the increase was dependent on the chosen model compound and the silica type. Silsol 6035 exhibited a greater extent of solubility improvement compared to the XDP 3050 formulations.

For CoQ10 the most significant impact on solubility in biorelevant medium was measured, with the maximum-loaded Silsol 6035 formulation exceeding the equilibrium solubility in biorelevant medium of 5.5 μg/mL by a factor of 128 (703.3 μg/mL), while the maximum-loaded XDP 3050 formulation exceeded it by a factor of 107 (588.6 μg/mL) (Fig. 4**A**). Notably, the XDP 3050 formulations with 1–15 % (*w/w)* CoQ10 drug load did not impact solubility. However, only the 1 % loaded formulation of Silsol 6035 achieved no effect. Due to the high matrix content of the ASX-enriched oleoresin, lower drug loads were achieved compared to CoQ10 (0.1 – 5.9 %). Nevertheless, all loaded silica formulations improved solubility, except for the one with 0.1 %

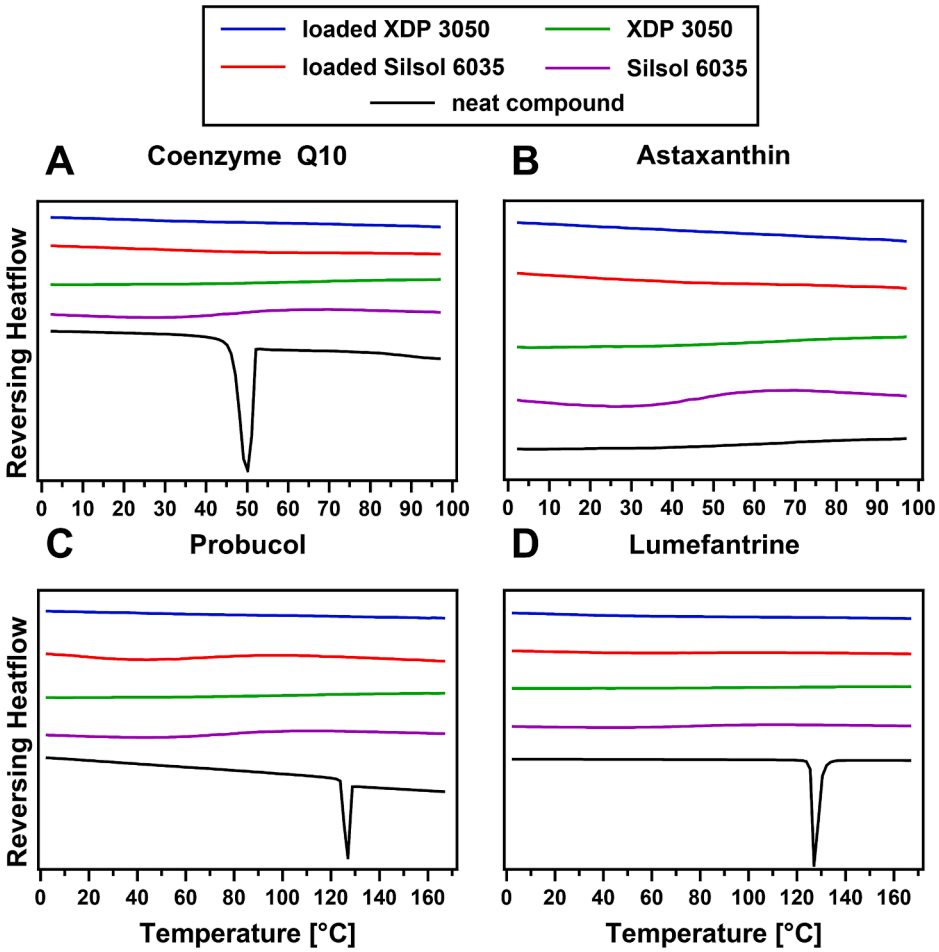


**Fig. 2.** DSC thermograms (exo up) of coenzyme Q10 (A), astaxanthin (B), probucol (C), lumefantrine (D), XDP 3050, Silsol 6035 and the mesoporous silica formulations with the highest achievable drug load.

drug load (Fig. 4**B**). The 5 % loaded XDP 3050 formulation showed the greatest increase in solubility (180x; 198.3 μg/mL), while Silsol 6035 showed a maximal solubility improvement by a factor of 93 (102.4 μg/mL). For PB, the 1 %-loaded silica formulations did not impact solubility, while positive results were observed for all other drug loads. Silsol 6035 showed an improvement factor of 128 (255.3 μg/mL), whereas XDP 3050 improved the solubility of PB by a factor of 108 (215.1 μg/mL) (Fig. 4**C**). LU formulations exhibited the least impact on solubility improvement in the biorelevant medium. Only the maximum loaded formulation of XDP 3050 achieved an effect, resulting in an improvement by a factor of 20 (73.8 μg/mL). Silsol 6035 performed better, with a maximum improvement factor of 35 (41.9 μg/mL) (Fig. 4**D**).

Besides the loading quantity of the silica carrier particles, the model compound solubility in biorelevant medium was additionally influenced by the amount of loaded silica formulation per solvent volume. This correlation was exemplarily investigated for the CoQ10 - XDP 3050 and Silsol 6035 formulations with the highest possible drug load (Fig. 5). When the formulation quantity per mL increased, the concentration of CoQ10 in solution increased linearly for both types of silica. However, this effect was more pronounced for XDP 3050, resulting in significantly higher CoQ10 concentrations in solution when compared to loaded Silsol 6035 of the same formulation quantity. The difference in CoQ10 concentration achieved in solution by both mesoporous carriers thereby raised notably with increasing formulation quantity.

### 3.5. Apparent solubility/ kinetic concentration

Solvent shift experiments were conducted to investigate the apparent solubility (i.e., kinetic concentration) of the model compounds (Fig. 6). CoQ10, PB, and LU exhibited comparable solubility profiles. At the beginning of the measurements, the concentration was 18–28 times higher than the equilibrium solubility. However, over time, the concentration decreased due to precipitation of the dissolved active ingredient. As a result, after 270 min, the concentration of the dissolved active ingredient reached its lowest point. Nevertheless, the concentration remained still above the equilibrium solubility (Table 3). The presence of additionally suspended XDP 3050 or Silsol 6035 in the aqueous medium had no effect on the concentration profile (**Figure S1**).

CoQ10 achieved the highest concentration of all the tested model compounds. Compared to the crystalline drug, solubility was increased 18.7-times after 6 min, reaching 103 μg/mL. However, the concentration gradually decreased to 69.5 μg/mL after 270 min (Fig. 6**A**). Due to the paste-like consistency at room temperature of the ASX enriched oleoresin, it formed large droplets immediately after the solvent shift, resulting in ASX concentration of approximately 1 μg/mL throughout the experiment (Fig. 6**B**). The concentration of PB reached 56.6 μg/mL after 6 min, which represented a 28.3-fold increase compared to the crystalline substance. The concentration decreased to 38.9 μg/mL during the experiment (Fig. 6**C**). The solubility of LU improved by a factor of 17.5, achieving a concentration of 36.7 μg/mL (6 min), with a subsequent gradual decreased to 30.0 μg/mL (Fig. 6**D**).

### 3.6. Monophasic non-sink dissolution

The apparent solubility profiles obtained by solvent shift experiments were compared with monophasic non-sink dissolution profiles in

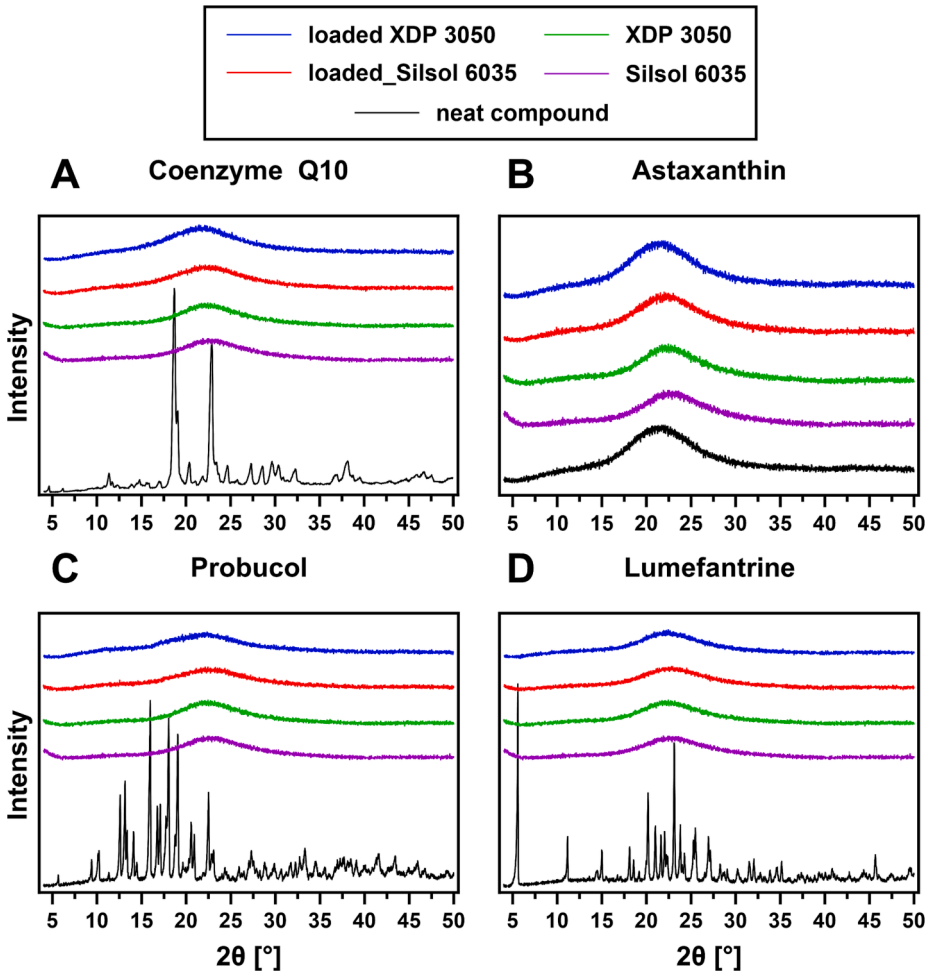


**Fig. 3.** X-ray powder diffraction (XRPD) diffractograms of coenzyme Q10 (A), astaxanthin (B), probucol (C), lumefantrine (D), XDP 3050, Silsol 6035 and the mesoporous silica formulations with the highest achievable drug load.

biorelevant medium (using the BiPHa + apparatus without the organic absorption sink). Since, the results of the shake flask experiments revealed that the solubility of the model compounds increased with increasing drug load, only the formulations with the highest possible drug load were evaluated.

The results showed that there was a substantial increase in the release rate of CoQ10 generated by the loaded XDP 3050 and Silsol 6035 formulations, when compared to the crystalline compound. The concentration of CoQ10 increased rapidly for both formulations, with 80.3 μg/mL being released for loaded XDP 3050 and 34.4 μg/mL for loaded Silsol 6035 already after 60 min, thereby notably exceeding the equilibrium solubility of 5.5 μg/mL (Fig. 6**A**). However, during the measurements the release rate decreased notably, and the concentration of CoQ10 increased only slowly. After 270 min, XDP 3050 released 93.0 μg/mL of CoQ10, while Silsol 6035 released 43.2 μg/mL. For the XDP 3050 formulation, the concentration of CoQ10 at the end of the dissolution measurement closely matched the apparent/amorphous solubility observed in the solvent shift experiment.

Mesoporous silica loaded with the ASX enriched oleoresin showed similar effects compared to CoQ10. The release rate was initially high but decreased over time, reaching a plateau already after 60 min (Fig. 6**B**). The XDP 3050 formulation showed a release of 58.0 μg/mL, while the Silsol 6035 formulation had a release of 23.6 μg/mL. Both concentrations were decisively higher than the equilibrium solubility of ASX in biorelevant medium (1.1 μg/mL). However, unlike CoQ10, both loaded silica formulations surpassed the apparent solubility of ASX measured in the solvent shift experiment. In addition, there was no evidence of extract precipitation or droplet formation.

During investigation of the PB and LU formulations, it was observed that the silica formulations of both APIs did not achieve the same release rates as the CoQ10 and ASX formulations (Fig. 6**C/D**). After 270 min, only low concentrations, which were well below the apparent solubility, were observed and no rapid release kinetics could be detected. Instead, a slow release with steadily increasing PB and LU concentrations was observed. Nevertheless, the equilibrium solubility had already been exceeded after 120 min for both active ingredients. The PB-loaded XDP 3050 reached 6.3 μg/mL after 270 min, and PB-loaded Silsol 6035 reached 13.7 μg/mL. This represented an increase by 3.2–6.9 compared to the unformulated compound. XDP 3050 and Silsol 6035 formulations loaded with LU increased solubility by a factor of 4.1–2.7 and achieved 8.7 μg/mL and 5.6 μg/mL, respectively.

In general, for all model compounds, the measured concentration of active substance in solution remained stable over a period of 24 h and no precipitation was observed (**Figure S2**).

### *3.7. Interaction of the model compounds with the silica surface*

To assess the extent of molecular interactions between the different model compounds and amorphous silica, COSMOquick calculations of the enthalpy of mixing $\Delta H_{mix}$ and TLC experiments (Table 5) were carried out.

Comparable values for $\Delta H_{mix}$ ranging from −9.25 to −12.68 kJ/mol were obtained for ASX, LU, and PB. However, a notably lower enthalpy of −4.35 kJ/mol was calculated for CoQ10. In contrast, TLC analysis

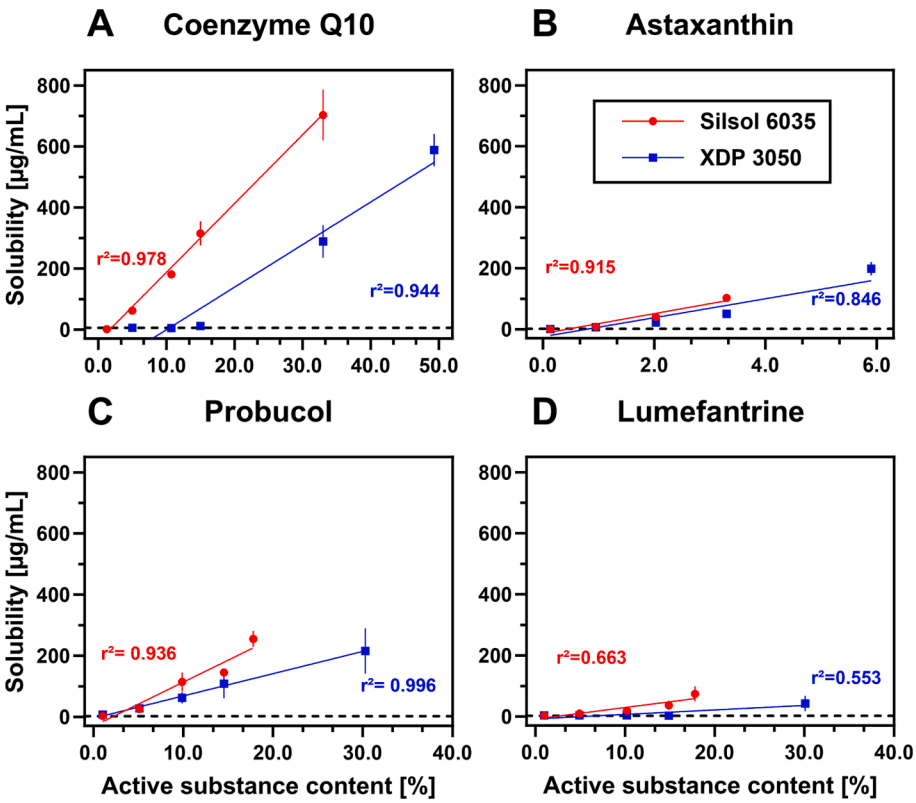


**Fig. 4.** Drug load-dependent equilibrium solubility (determined by HPLC) of coenzyme Q10 (A), astaxanthin (B), probucol (C) and lumefantrine (D) loaded mesoporous silica (XDP 3050/ Silsol 6035) in biorelevant medium (20.0 mL Bi-FaSSIF-V2, pH 6.8); $n = 6$; the dashed line represents the equilibrium solubility (48 h) of the neat compounds (determined by shake flask method).

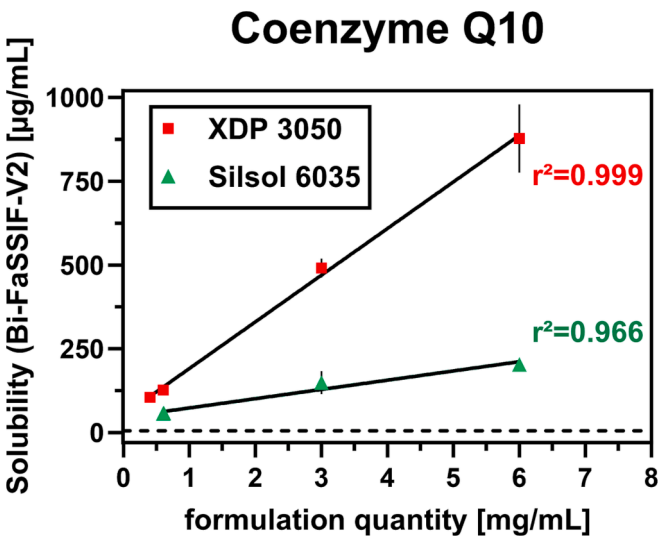


**Fig. 5.** Evaluation of the effect of formulation quantity of maximum loaded coenzyme Q10 (CoQ10) – XDP 3050 /Silsol 6035 formulations on CoQ10 equilibrium solubility (determined by HPLC) in biorelevant medium (20.0 mL Bi-FaSSIF-V2, pH 6.8) determined by shake flask experiments; $n = 6$; the dashed line represents the equilibrium solubility of the neat compound after 48 h (determined by shake flask method).

revealed comparable Rf-values of 0.85 to 0.89 for CoQ10, ASX, and PB, while for LU exhibited a lower value of 0.40.

### 3.8. *Biorelevant biphasic dissolution*

Similar to the results obtained from shake flask experiments, it was found that with increasing drug load of the silica formulations an increase in model compound concentration in the 1-decanol absorption sink of the BiPHa + biorelevant biphasic dissolution was overserved (Figure S4). Therefore, only the formulations with the highest drug load were examined in terms of their dissolution behavior.

Loading of CoQ10 onto XDP 3050 enhanced the water solubility of CoQ10 and 22.3 % release was detected after 30 min (Fig. 7**A**). The self-emulsifying micellar formulation (1. commercial formulation for comparison), however, was the most effective at optimizing water solubility. It released 70 % of the active ingredient in the first 30 min. The oily dispersion formulations (2. commercial formulation for comparison) and Silsol 6035 showed no improvement in solubility compared to unformulated CoQ10, that reached a concentration of 2.0 % after 270 min. Focusing on the 1-decanol absorption sink, the mesoporous silica formulations demonstrated a pronounced increase in partitioning rate when compared to unformulated CoQ10 and both market formulations (Fig. 7**B**). Pure CoQ10 reached an end concentration of 1.5 % in 1-decanol (270 min), the two market formulations achieved 3.6–4.0 %, representing an increase by a factor of 2.4 to 2.7. In contrast, the silica formulations reached decisively higher concentrations. For the loaded Silsol 6035 formulation, in the organic medium a CoQ10 concentration of 15.3 % was measured after 270 min, which represented a 10-fold increase compared to pure active ingredient and a 3.8 to 4.3 increase compared to the market formulations. The formulation containing XDP 3050 reached the highest CoQ10 concentration among all formulations tested, measuring 18.4 % in the 1-decanol layer. This displayed a five-

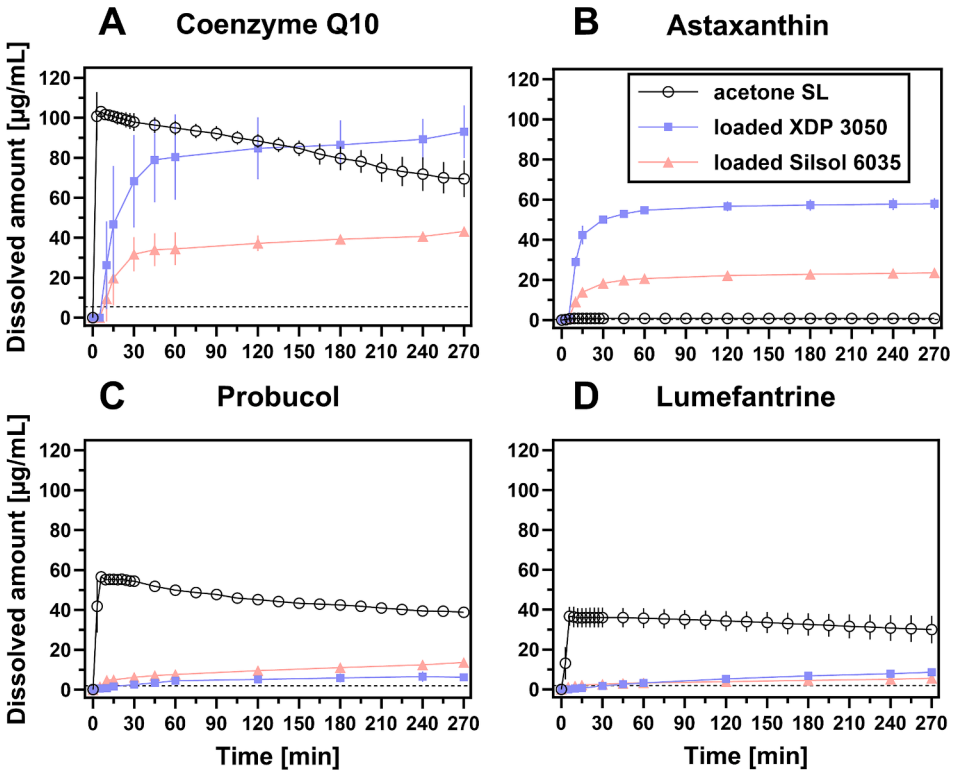


**Fig. 6.** Apparent solubility/ kinetic concentrations in biorelevant medium (50.0 mL Bi-FaSSIF-V2, pH 6.8) of neat coenzyme Q10 (A), astaxanthin (B), probucol (C), lumefantrine (D) and monophasic non-sink dissolution profiles of their corresponding loaded silica formulations, (100 % corresponds to 200 µg/mL); $n = 3$; the dashed line represents the equilibrium solubility (48 h) of the neat compounds (determined by shake flask method).

**Table 5**
Rf-values and COSMOquick enthalpy of mixing at 37 °C obtained for coenzyme Q10, astaxanthin, probucol and lumefantrine.

| Active ingredient | Rf-Value | $\Delta H_{mix}$ [kJ/mol] |
|---|---|---|
| Coenzyme Q10 | 0.85 | − 4.35 |
| Astaxanthin | 0.88 | − 12.68 |
| Probucol | 0.89 | − 9.63 |
| Lumefantrine | 0.40 | − 9.25 |

fold increase compared to the commercial formulations.

Regarding the ASX formulations, both mesoporous silica carriers demonstrated an increase in ASX solubility in the aqueous dissolution medium (Fig. 7**C**). The concentration profiles were comparable, with peak concentrations of 4.6 % detected after 30 min. In contrast, the unformulated extract reached minimal dissolution in water and maintained a concentration below 1 % throughout the dissolution measurement. The self-emulsifying micellar formulation (commercial formulation for comparison) dissolved quickly and completely, achieving 90 % release after 30 min. In the organic phase, only the silica formulations exhibited a notable increase in partitioning rate and concentration, with ASX concentrations of 6.0 % being measured for the XDP 3050 formulation and 5.7 % for the Silsol 6035 formulation after 270 min (Fig. 7**D**). Neither the unformulated extract nor the micelles were able to achieve end concentrations higher than 1 %. Thus, the silica formulations improved ASX partitioning into the organic absorption sink by 8 to 15 times compared to the market formulation.

For PB and LU no reference commercial formulations were available. Thus, the unformulated active ingredients were used for comparison. Both mesoporous silica formulations improved the water solubility and partitioning rate of PB and LU. However, the effects were less pronounced compared to CoQ10 and ASX.

Regarding formulations containing PB, the use of Silsol 6035 as a carrier led to an increase in concentration in the aqueous medium and after the addition of biorelevant surfactants (30 min), the concentration reached 17.3 % (Fig. 8**A**). Subsequently, a reduction to 8.9 % was observed. The unformulated active ingredient only reached 1 % after 30 min, which further decreased to 0.5 %. For loaded XDP 3050 only a minor increase in solubility was detected, with a measurement of 5.2 % PB in the aqueous medium after 30 min. In the organic medium however, both silica formulations enhanced the partitioning rate, with XDP 3050 and Silsol 6035 achieving PB concentration of 2.3 % and 2.7 % (270 min), respectively (Fig. 8**B**). This corresponded to a five-fold increase compared to unformulated PB, which reached 0.5 % at the end of the biorelevant dissolution test. Although the Silsol 6035 formulation increased the concentration of PB in the aqueous medium, it did not show an improvement in partitioning rate compared to the XDP 3050 formulation.

Results from the dissolution measurements of LU indicated only minor improvements in aqueous solubility and partitioning rate into the organic phase for loaded Silsol 6035 and XDP 3050. Nonetheless, the Silsol 6035 formulation exhibited an increase in the maximum LU concentration in the aqueous medium from 1.8 % (measured for unformulated LU) to 8.0 % after the addition of biorelevant surfactants (Fig. 8**C**). The concentration gradually decreased to 4.1 % throughout the test. In contrast, using XDP 3050 as a carrier had a reduced impact on LU solubility, with a concentration of 4.3 % measured after 30 min, which subsequently decreased to 2.1 %. In comparison to the PB formulations, the enhanced solubility of LU led to a greater partitioning rate into the 1-decanol layer (Fig. 8**D**). After 270 min, 3.0 % and 2.1 % were measured for the Silsol 6035 and XDP 3050 formulations, respectively. This represented an improvement of 3 and 2.1 compared to unformulated LU, which reached a concentration of 1.0 %.

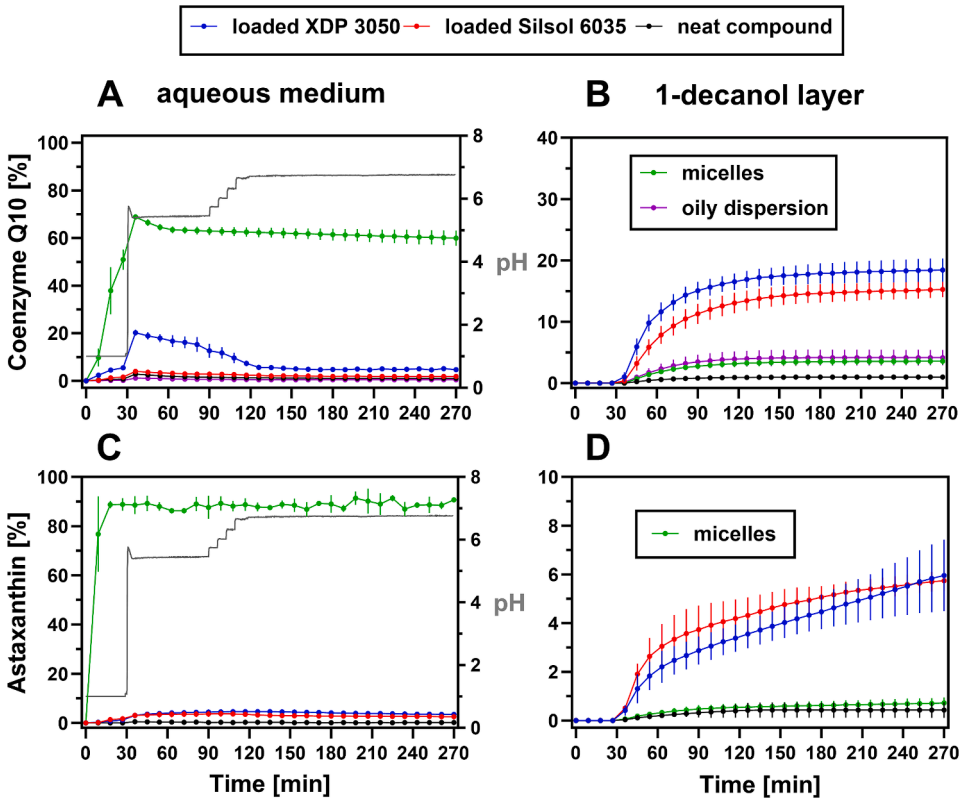


**Fig. 7.** Released/ partitioned amount of coenzyme Q10 (including micelles and oily dispersion as reference commercial formulation with previously studied bioavailability (Schulz et al., 2006)) and astaxanthin (including micelles as reference commercial formulation) (mean ± SD); coenzyme Q10 aqueous medium (A), coenzyme Q10 1-decanol layer (B), astaxanthin aqueous medium (C), astaxanthin 1-decanol layer (D); the pH profile in the aqueous medium is represented by the grey line, (100 % corresponds to 200 μg/mL); n = 6.

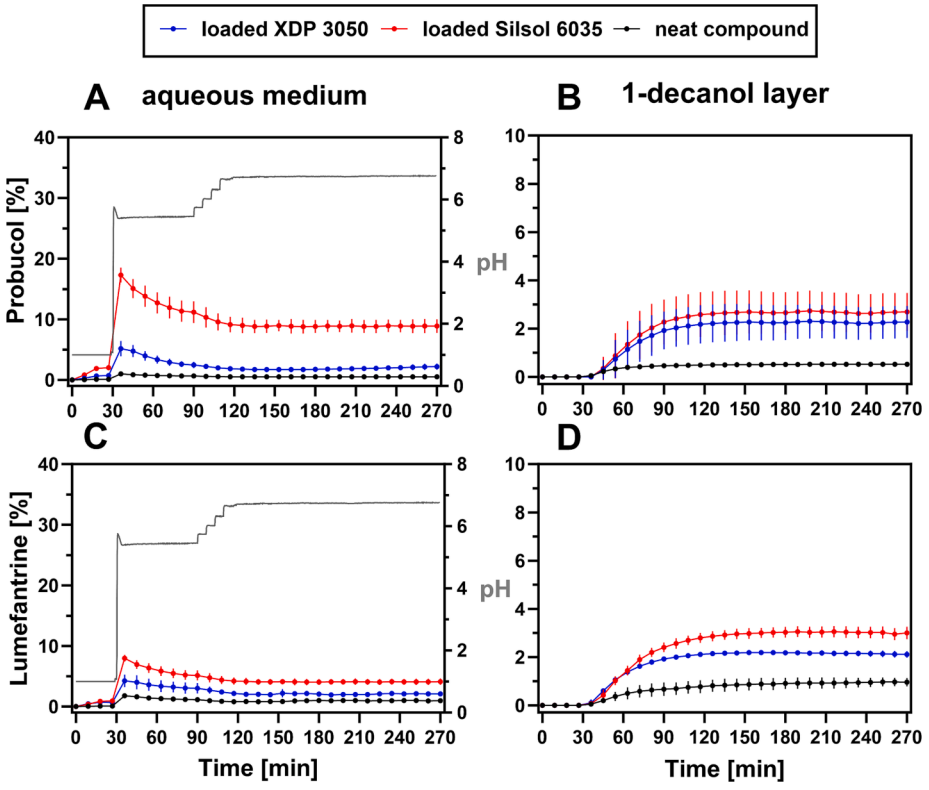


**Fig. 8.** Released/ partitioned amount of probucol and lumefantrine (mean ± SD); probucol aqueous medium (A), probucol 1-decanol layer (B), lumefantrine aqueous medium (C), lumefantrine 1-decanol layer (D); the pH profile in the aqueous medium is represented by the grey line, (100 % corresponds to 200 μg/mL); $n = 6$.

## 4. Discussion

In the current study, we investigated how the drug load of the manufactured mesoporous silica formulations impacted solubility in various media and biorelevant biphasic dissolution performance. For this purpose, four highly lipophilic and poorly soluble natural products and synthetic APIs were chosen as model compounds. Despite the structural diversity of the model compounds, with increasing drug load a distinct improvement in solubility in biorelevant medium was observed, greatly surpassing the equilibrium solubility and improving biorelevant biphasic dissolution performance.

### 4.1. Investigation of the solid state

At very high drug loads of up to 50 % (*w/w*), both mesoporous silica carriers could stabilize all model compounds in a non-crystalline form, as DSC and XRPD measurements after manufacturing of the formulations revealed no remaining crystallinity (Fig. 2 and Fig. 3). Mesoporous carriers are known for their ability to inhibit crystallization processes of drugs by confining them in their internal ordered pore structure with nanopores in a diameter range of 2–30 nm, especially if the pore size is comparable to the critical nuclei size (Dening and Taylor, 2018; Vraníková et al., 2020). According to the theory of homogeneous nucleation, only nuclei larger than a critical nucleation size can grow and cause formulation instability. If the pore size is smaller than about 12 times the molecular size of the drug, it is estimated that drug would be sufficiently confined in the nanopores to remain in a non-crystalline form (Shen et al., 2017). XDP 3050 and Silsol 6035 have an averaged pore diameter of 22.9 nm and 6.0 nm, respectively. Considering the relatively large molecular dimensions of the model compounds (MW of up to 860 g/mol; see Table 3), the space in the mesopores was insufficient for crystallization to occur and the model compounds remained in a non-crystalline state. Usually, a monomolecular surface coverage of the silica particles is targeted to harness the molecular interactions with the silica surface. However, Le et al. showed that depending on the investigated API 200 to 300 % surface coverage could be achieved, while still preventing drug recrystallization (Le et al., 2019). In addition, Hate et al. achieved non-crystalline formulations of atazanavir loaded mesoporous SBA-15 with drug loads of up to 50 % (*w/w*) (Hate et al., 2020). Even with multi-layer adsorption of drug within the pores, the mechanism of nanoconfinement could prevented recrystallization (Antonino et al., 2019).

### 4.2. Solubility behavior

Unlike the crystalline form, dissolving non-crystalline material does not involve breaking the crystal lattice structure. This enhances interactions with solvent molecules, resulting in an exceedance of the thermodynamic solubility (Singh and Van den Mooter, 2016). Consequently, loaded silica formulations exhibited notably increased equilibrium solubility (Fig. 4). The ability to generate supersaturated solutions is described in the literature for a variety of different silica and active ingredients (Dening and Taylor, 2018; Ditzinger et al., 2019b; Le et al., 2019; Price et al., 2019). However, depending on the model compound and silica carrier used, a drug load dependent threshold value below which no improvement in equilibrium solubility occurred was observed. This might be related to the formation of a dynamic adsorption equilibrium between the silica surface and the drug molecules. Dening and Taylor described adsorption of ritonavir to SBA-15, which was used as a mesoporous carrier, as the reason for the incomplete release of ritonavir from these formulations (Dening and Taylor, 2018). Assuming that a model compound and silica specific amount of active ingredient would remain adsorbed on the silica surface, increased drug load could compensate for the adsorbed fraction and increase dissolution. An ingress of water may lead to competitive interactions of active ingredient with water molecules on the silica surface, leading to a displacement of active ingredient. If non-crystalline active ingredient is released from the mesopores, it could be directly solubilized by the surfactants lecithin und taurocholate present in the biorelevant medium. Hereby, the released fraction is stabilized in solution, even at high concentrations. Thus, an increased degree of turbidity of the aqueous medium was observe for the highly loaded silica formulations. However, if surfactant-free medium such as phosphate buffer was used, the released active ingredient could not be stabilized in solution and precipitation occurred (**Table S1** and **Tabel S2**).

The differences in model compound concentration observed between both mesoporous silica carriers can be attributed to their differing pore sizes. The smaller pores of Silsol 6035 (6 nm) enabled for equally high concentrations already at lower drug loads, when compared to XDP 3050 with an average pore size of 23 nm. The higher capillary forces in the smaller pores of Silsol 6035 promoted the ingress of water and the competitive displacement of active ingredient from the silica surface. However, the extent of the solubility improvement strongly depended on the model compound studied, with CoQ10 showing the greatest effect. The differences in equilibrium solubility improvement might be explained by the strength of interaction between the model compounds and the silica surface on the one hand, and the interactions between the drug molecules themselves (i.e., self-cohesion) on the other hand. The strength of interaction is represented by the enthalpy of mixing $\Delta H_{mix}$ (Table 5). CoQ10 had a significantly lower enthalpy of −4.35 kJ/mol compared to the other model compounds, indicating a higher tendency to be brought in solution. In addition, CoQ10 showed the highest apparent solubility (Fig. 6). Conversely, the lowest equilibrium solubility-enhancing effect among all formulations was observed for LU. TLC experiments revealed a lower Rf value of 0.40, indicating a stronger interaction with the silica surface compared to the other model compounds (Rf value between 0.85 and 0.89) (Table 5). In addition, (with the exception of the semi-solid ASX oleoresin) LU showed the lowest apparent solubility. The combined estimation of molecular drug-silica interactions by the theoretical calculations together with the chromatographic screening method appears to be a promising approach. While the binary $\Delta H_{mix}$ calculations were based on sound quantum-chemical and thermodynamic level of theory, the values were based on simplified binary drug-silica interactions in the bulk, while the water phase on the surface was neglected. Therefore, $\Delta H_{mix}$ can be considered as a measure of intrinsic drug affinity to silica. This was complemented with the chromatographic screening method in which a mobile phase was present to capture further effects of solvation or possible ionization such as possibly for LU.

### 4.3. Mono- and biphasic dissolution results

In line with the shake flask experiments, all silica formulations showed increased mono- and biphasic dissolution performance at the investigated dose of 10 mg active ingredient per vessel (Fig. 6). A similar behavior was observed by Price et al. who found a rapid release kinetic for non-crystalline dipyridamole, glibenclamide and fenofibrate loaded onto mesoporous Parteck SLC (Price et al., 2019). However, monophasic dissolution studies resulted in significantly lower concentrations for all model compounds when compared to the 48 h shake flask measurements. This discrepancy could be attributed to the fact that the model compound concentration depended not only on the drug load, but also on the amount of formulation per volume of dissolution medium (Fig. 5). The extent of increase varied based on the mesoporous silica type used, which explains the lower concentration measured in the aqueous medium during CoQ10 - Silsol 6035 dissolution experiments compared to XDP 3050, although shake flask experiments had shown a greater solubility enhancing effect for Silsol 6035. During the shake flask experiments, a notably larger excess of formulation was used. In addition to the active ingredient, the silica carrier particles themselves also dissolve partially (up to 120 ppm), which in turn can influence the dissolution behavior of the active ingredient. Indeed, saturation of the solvent with

silica was previously reported to have a significant effect on drug release (Andersson et al., 2004). However, the dependence of this effect on the structural properties of the active ingredient and mesoporous silica carrier still requires further investigation.

Biorelevant biphasic dissolution with proven *in vivo* relevance not only for synthetic APIs (Denninger et al., 2023, 2021) but also for natural products (Brenner et al., 2023), was used to ruffly estimate the *in vivo* performance of the highly loaded silica formulations in comparison to currently available commercial formulations. Since preliminary results based on CoQ10 – XDP 3050 formulations revealed an increase in dissolution performance with increasing drug load (**Figure S4**), only the formulations with the highest possible drug load were tested. An increase in the concentration in the organic phase was to be expected, as only dissolved active ingredient is available for partitioning into the organic medium (Brenner et al., 2023).

Although the silica formulations of CoQ10 and ASX released lower amounts of active ingredient in the aqueous medium compared to the self-emulsifying commercial formulations (Fig. 7), they showed notably higher partitioning rates into the organic absorption sink than all other formulations. The increased partitioning rate compared to the commercial formulations may be attributed to the quick release kinetic of active ingredient from the mesopores after adding biorelevant surfactants (refer to Fig. 6). As a result, CoQ10 and ASX become readily available for transfer into the organic phase, reducing the concentration of the active ingredient in the water phase. This stimulates more active ingredient to be released from the reservoir in the mesopores, creating a dynamic equilibrium that allows for a high partitioning rate into the organic phase while maintaining a low absolute concentration of active ingredient in the aqueous medium. Denninger et al. also discovered that ritonavir demonstrated a high partitioning rate in the organic phase, while its concentration in the aqueous medium remained low (Denninger et al., 2020). By contrast, the micellar inclusion complexes formed by the self-emulsifying formulations were too stable to allow for sufficient transfer of CoQ10 or ASX into the organic absorption sink (Miller et al., 2011). The *in situ* formed micelles entrapped the active ingredient and therefore, the amount of free drug available for partitioning into the organic layer was limited (Locher et al., 2016).

Compared to CoQ10 and ASX, for the PB and LU formulations reduced improvements were observed (Fig. 8). This initially seems surprising, as the PB-Silsol 6035 formulation notably improved water solubility. However, it is likely that the formation of stable micellar inclusion complexes with the biorelevant surfactants lecithin and taurocholate hindered partitioning across the aqueous/organic interface, which resulted in a decrease in PB accumulation in the organic absorption sink. Accordingly, even when dissolution of a supersaturated PB solution was studied, only a minor increase in partitioning rate was achieved (**Figure S5**). Nevertheless, an increase in the partitioning rate was observed for both PB and LU loaded silica formulations. The low solubility-enhancing effect of the loaded silica formulations, in combination with a slow release kinetic, might explain the less pronounced increase in partitioning rate of LU. Active ingredient that was removed from the aqueous medium through partitioning into the organic absorption sink could only be replenished slowly from the reservoir inside the mesoporous silica particles.

Due to their very high lipophilicity (log $D_{7.4} > 8$; see Table 3), all model compounds had an extremely low affinity to water and therefore, only insufficient concentrations were reached during dissolution experiments. Consequently, surfactants were necessary to achieve sufficient active substance concentrations in solution. Lecithin and taurocholate were available as biorelevant surfactants in the dissolution medium and differences in such mixed micelle partitioning likely contributed to a less optimal dissolution enhancement of PB and LU (see Fig. 7 and Fig. 8) compared to CoQ10 and ASX.

## 5. Conclusion

Highly loaded mesoporous silica particles represented an excellent formulation approach for very lipophilic, poorly soluble active ingredients. The presented method enabled the formulations to have high drug loads of up to 50 % (*w/w*), while still stabilizing the active ingredients in a non-crystalline form. Furthermore, the formulations greatly enhanced the solubility of the active ingredients in biorelevant medium, leading to improved performance during biorelevant biphasic dissolution studies. Particularly the natural products CoQ10 and ASX showed substantial benefits from being loaded onto mesoporous carrier particles and clearly outperformed currently available commercial formulations. This paper introduced the calculation of a mixing enthalpy for drug and silica as well as an experimental chromatographic method to estimate molecular interactions between drug and carrier. The given *in silico* approach was meant to characterize an intrinsic affinity of drug to silica, whereas the chromatographic method had a mobile phase that complemented the calculations by capturing possible effects of solvation and ionization in solution phase. The usefulness of these pre-formulation approaches would have to be demonstrated with further compounds to draw firm conclusions. Further investigations are also required to unveil the detailed mechanistic relationships between the interactions of the mesoporous silica particles and various structurally different APIs as well as performance evaluation *in vivo*.

**Funding**.

This research did not receive any specific grant from funding agencies in the public, commercial, or not-for-profit sectors.

## CRediT authorship contribution statement

**Marvin Benedikt Brenner:** Conceptualization, Data curation, Investigation, Methodology, Visualization, Writing – original draft. **Matthias Wüst:** Resources, Validation, Writing – review & editing. **Martin Kuentz:** Investigation, Methodology, Writing – review & editing. **Karl G. Wagner:** Conceptualization, Resources, Supervision, Writing – review & editing.

## Declaration of competing interest

The authors declare that they have no known competing financial interests or personal relationships that could have appeared to influence the work reported in this paper.

## Data availability

Data will be made available on request.

## Acknowledgements

The graphical abstract was created with Biorender.com.

## Appendix A. Supplementary data

Supplementary data to this article can be found online at https://doi.org/10.1016/j.ijpharm.2024.123946.

## References

Andersson, J., Rosenholm, J., Areva, S., Lindén, M., 2004. Influences of material characteristics on ibuprofen drug loading and release profiles from ordered micro- and mesoporous silica matrices. Chem. Mater. 16, 4160–4167. https://doi.org/10.1021/cm0401490.

Antonino, R.S.C.M.Q., Ruggiero, M., Song, Z., Nascimento, T.L., Lima, E.M., Bohr, A., Knopp, M.M., Löbmann, K., 2019. Impact of drug loading in mesoporous silica-amorphous formulations on the physical stability of drugs with high recrystallization tendency. Int. J. Pharm. X 1, 100026. https://doi.org/10.1016/j.ijpx.2019.100026.

Atriya, A., Majee, C., Mazumder, R., Choudhary, A.N., Salahuddin, Mazumder, A., Dahiya, A., Priya, N., 2023. Insight into the various approaches for the enhancement

of bioavailability and pharmacological potency of terpenoids: a review. Curr. Pharm. Biotechnol. 24, 1228–1244. https://doi.org/10.2174/1389201024666221130163116.
Baghel, S., Cathcart, H., O'Reilly, N.J., 2016. Polymeric amorphous solid dispersions: a review of amorphization, crystallization, stabilization, solid-state characterization, and aqueous solubilization of biopharmaceutical classification system class II drugs. J. Pharm. Sci. 105, 2527–2544. https://doi.org/10.1016/j.xphs.2015.10.008.
Barthe, L., Woodley, J., Houin, G., 1999. Gastrointestinal absorption of drugs: methods and studies. Fundam. Clin. Pharmacol. 13, 154–168. https://doi.org/10.1111/j.1472-8206.1999.tb00334.x.
Bookwala, M., Wildfong, P.L.D., 2023. The implications of drug-polymer interactions on the physical stability of amorphous solid dispersions. Pharm. Res. https://doi.org/10.1007/s11095-023-03547-4.
Brenner, M.B., Flory, S., Wüst, M., Frank, J., Wagner, K., 2023. Novel biphasic in vitro dissolution method correctly predicts the Oral bioavailability of curcumin in humans. J. Agric. Food Chem. https://doi.org/10.1021/acs.jafc.3c04990.
Brouwers, J., Brewster, M.E., Augustijns, P., 2009. Supersaturating drug delivery systems: the answer to solubility-limited Oral bioavailability? J. Pharm. Sci. 98, 2549–2572. https://doi.org/10.1002/jps.21650.
Cokenakes, G., 2021. Liquid imbibition into mesoporous silica. University of the Sciences, Philadelphia.
Dening, T.J., Taylor, L.S., 2018. Supersaturation potential of ordered mesoporous silica delivery systems. part 1: dissolution performance and drug membrane transport rates. Mol. Pharm. 15, 3489–3501. https://doi.org/10.1021/acs.molpharmaceut.8b00488.
Denninger, A., Westedt, U., Rosenberg, J., Wagner, K.G., 2020. A rational Design of a Biphasic DissolutionSetup-modelling of biorelevant kinetics for a ritonavir hot-melt extruded amorphous solid dispersion. Pharmaceutics 12. https://doi.org/10.3390/pharmaceutics12030237.
Denninger, A., Westedt, U., Wagner, K.G., 2021. Shared IVIVR for five commercial enabling formulations using the BiPHa+ biphasic dissolution assay. Pharmaceutics 13. https://doi.org/10.3390/pharmaceutics13020285.
Denninger, A., Becker, T., Westedt, U., Wagner, K.G., 2023. Advanced in vivo prediction by introducing biphasic dissolution data into PBPK models. Pharmaceutics 15, 1978. https://doi.org/10.3390/pharmaceutics15071978.
Descamps, M., Willart, J.-F., 2018. Scaling laws and size effects for amorphous crystallization kinetics: constraints imposed by nucleation and growth specificities. Int. J. Pharm. 542, 186–195. https://doi.org/10.1016/j.ijpharm.2018.03.001.
Ditzinger, F., Price, D.J., Ilie, A.-R., Köhl, N.J., Jankovic, S., Tsakiridou, G., Aleandri, S., Kalantzi, L., Holm, R., Nair, A., Saal, C., Griffin, B., Kuentz, M., 2019a. Lipophilicity and hydrophobicity considerations in bio-enabling oral formulations approaches – a PEARRL review. J. Pharm. Pharmacol. 71, 464–482. https://doi.org/10.1111/jphp.12984.
Ditzinger, F., Price, D.J., Nair, A., Becker-Baldus, J., Glaubitz, C., Dressman, J.B., Saal, C., Kuentz, M., 2019b. Opportunities for successful stabilization of poor glass-forming drugs: a stability-based comparison of mesoporous silica versus hot melt extrusion technologies. Pharmaceutics 11, 577. https://doi.org/10.3390/pharmaceutics11110577.
du Plessis, L.H., Govender, K., Denti, P., Wiesner, L., 2015. In vivo efficacy and bioavailability of lumefantrine: evaluating the application of pheroid technology. Eur. J. Pharm. Biopharm. 97, 68–77. https://doi.org/10.1016/j.ejpb.2015.10.001.
Gershkovich, P., Hoffman, A., 2005. Uptake of lipophilic drugs by plasma derived isolated chylomicrons: linear correlation with intestinal lymphatic bioavailability. Eur. J. Pharm. Sci. 26, 394–404. https://doi.org/10.1016/j.ejps.2005.07.011.
Hate, S.S., Reutzel-Edens, S.M., Taylor, L.S., 2020. Interplay of adsorption, supersaturation and the presence of an absorptive sink on drug release from mesoporous silica-based formulations. Pharm. Res. 37, 163. https://doi.org/10.1007/s11095-020-02879-9.
International council for harmonisation, 2021. Impurities: Guidline for residual solvents Q3C (R8).
Jannel, S., Caro, Y., Bermudes, M., Petit, T., 2020. Novel insights into the biotechnological production of Haematococcus pluvialis-derived astaxanthin: advances and key challenges to allow its industrial use as novel food ingredient. J. Mar. Sci. Eng. 8, 789. https://doi.org/10.3390/jmse8100789.
Janssens, S., Van den Mooter, G., 2009. Review: physical chemistry of solid dispersions. J. Pharm. Pharmacol. 61, 1571–1586. https://doi.org/10.1211/jpp.61.12.0001.
Karagianni, A., Kachrimanis, K., Nikolakakis, I., 2018. Co-amorphous solid dispersions for solubility and absorption improvement of drugs: composition, preparation, characterization and formulations for Oral delivery. Pharmaceutics 10, 98. https://doi.org/10.3390/pharmaceutics10030098.
Knapik, J., Wojnarowska, Z., Grzybowska, K., Jurkiewicz, K., Stankiewicz, A., Paluch, M., 2016. Stabilization of the amorphous ezetimibe drug by confining its dimension. Mol. Pharm. 13, 1308–1316. https://doi.org/10.1021/acs.molpharmaceut.5b00903.
Le, T.-T., Elzhry Elyafi, A.K., Mohammed, A.R., Al-Khattawi, A., 2019. Delivery of poorly soluble drugs via mesoporous silica: impact of drug overloading on release and thermal profiles. Pharmaceutics 11, 269. https://doi.org/10.3390/pharmaceutics11060269.
Li, F., Li, L., Wang, S., Yang, Y., Li, J., Liu, D., Zhang, S., Wang, S., Xu, H., 2019a. Improved dissolution and oral absorption by co-grinding active drug probucol and ternary stabilizers mixtures with planetary beads-milling method. Asian J. Pharm. Sci. 14, 649–657. https://doi.org/10.1016/j.ajps.2018.12.001.
Li, Z., Zhang, Y., Feng, N., 2019b. Mesoporous silica nanoparticles: synthesis, classification, drug loading, pharmacokinetics, biocompatibility, and application in drug delivery. Expert Opin. Drug Deliv. 16, 219–237. https://doi.org/10.1080/17425247.2019.1575806.
Locher, K., Borghardt, J.M., Frank, K.J., Kloft, C., Wagner, K.G., 2016. Evolution of a mini-scale biphasic dissolution model: impact of model parameters on partitioning of dissolved API and modelling of in vivo-relevant kinetics. Eur. J. Pharm. Biopharm Off. J. Arbeitsgemeinschaft Pharm. Verfahrenstechnik EV 105, 166–175. https://doi.org/10.1016/j.ejpb.2016.06.008.
Loftsson, T., Brewster, M.E., 2010. Pharmaceutical applications of cyclodextrins: basic science and product development. J. Pharm. Pharmacol. 62, 1607–1621. https://doi.org/10.1111/j.2042-7158.2010.01030.x.
Loschen, C., Klamt, A., 2012. COSMOquick: a novel Interface for fast σ-profile composition and its application to COSMO-RS solvent screening using multiple reference solvents. Ind. Eng. Chem. Res. 51, 14303–14308. https://doi.org/10.1021/ie3023675.
Managuli, R.S., Raut, S.Y., Reddy, M.S., Mutalik, S., 2018. Targeting the intestinal lymphatic system: a versatile path for enhanced oral bioavailability of drugs. Expert Opin. Drug Deliv. 15, 787–804. https://doi.org/10.1080/17425247.2018.1503249.
Mano, C.M., Guaratini, T., Cardozo, K.H.M., Colepicolo, P., Bechara, E.J.H., Barros, M.P., 2018. Astaxanthin restrains nitrative-oxidative peroxidation in mitochondrial-mimetic liposomes: a pre-apoptosis model. Mar. Drugs 16, 126. https://doi.org/10.3390/md16040126.
Martinez, M.N., Amidon, G.L., 2002. A mechanistic approach to understanding the factors affecting drug absorption: a review of fundamentals. J. Clin. Pharmacol. 42, 620–643. https://doi.org/10.1177/00970002042006005.
McCarthy, C.A., Ahern, R.J., Devine, K.J., Crean, A.M., 2018. Role of drug adsorption onto the silica surface in drug release from mesoporous silica systems. Mol. Pharm. 15, 141–149. https://doi.org/10.1021/acs.molpharmaceut.7b00778.
Miao, F., Lu, D., Li, Y., Zeng, M., 2006. Characterization of astaxanthin esters in Haematococcus pluvialis by liquid chromatography–atmospheric pressure chemical ionization mass spectrometry. Anal. Biochem. 352, 176–181. https://doi.org/10.1016/j.ab.2006.03.006.
Miller, J.M., Beig, A., Krieg, B.J., Carr, R.A., Borchardt, T.B., Amidon, G.E., Amidon, G.L., Dahan, A., 2011. The solubility-permeability interplay: mechanistic modeling and predictive application of the impact of micellar solubilization on intestinal permeation. Mol. Pharm. 8, 1848–1856. https://doi.org/10.1021/mp200181v.
Mosca, F., Fattorini, D., Bompadre, S., Littarru, G.P., 2002. Assay of coenzyme Q10 in plasma by a single dilution step. Anal. Biochem. 305, 49–54. https://doi.org/10.1006/abio.2002.5653.
Neslihan Gursoy, R., Benita, S., 2004. Self-emulsifying drug delivery systems (SEDDS) for improved oral delivery of lipophilic drugs. Biomed. Pharmacother. 58, 173–182. https://doi.org/10.1016/j.biopha.2004.02.001.
Niederquell, A., Vraníková, B., Kuentz, M., 2023. Study of disordered mesoporous silica regarding intrinsic compound affinity to the carrier and drug-accessible surface area. Mol. Pharm. https://doi.org/10.1021/acs.molpharmaceut.3c00690.
Patel, K., Sarma, V., Vavia, P., 2013. Design and evaluation of lumefantrine – oleic acid self nanoemulsifying ionic complex for enhanced dissolution. DARU J. Pharm. Sci. 21, 27. https://doi.org/10.1186/2008-2231-21-27.
Pöstges, F., Kayser, K., Stoyanov, E., Wagner, K.G., 2022. Boost of solubility and supersaturation of celecoxib via synergistic interactions of methacrylic acid-ethyl acrylate copolymer (1:1) and hydroxypropyl cellulose in ternary amorphous solid dispersions. Int. J. Pharm. X 4, 100115. https://doi.org/10.1016/j.ijpx.2022.100115.
Price, D.J., Nair, A., Kuentz, M., Dressman, J., Saal, C., 2019. Calculation of drug-polymer mixing enthalpy as a new screening method of precipitation inhibitors for supersaturating pharmaceutical formulations. Eur. J. Pharm. Sci. 132, 142–156. https://doi.org/10.1016/j.ejps.2019.03.006.
Schulz, C., Obermüller-Jevic, U.C., Hasselwander, O., Bernhardt, J., Biesalski, H.K., 2006. Comparison of the relative bioavailability of different coenzyme Q10 formulations with a novel solubilizate (SoluTM Q10). Int. J. Food Sci. Nutr. 57, 546–555. https://doi.org/10.1080/09637480601058320.
Seljak, K.B., Kocbek, P., Gašperlin, M., 2020. Mesoporous silica nanoparticles as delivery carriers: an overview of drug loading techniques. J. Drug Deliv. Sci. Technol. 59, 101906 https://doi.org/10.1016/j.jddst.2020.101906.
Probucol: DrugBank Online. [WWW Document], n.d. URL https://go.drugbank.com/drugs/DB01599 (accessed 25.10.2023).
Shen, S.-C., Dong, Y.-C., Letchmanan, K., Ng, W.K., 2017. Chapter 23 - Mesoporous materials and technologies for development of oral medicine, in: Andronescu, E., Grumezescu, A.M. (Eds.), Nanostructures for Oral Medicine, Micro and Nano Technologies. Elsevier, pp. 699–749 10.1016/B978-0-323-47720-8.00024-9.
Singh, A., Van den Mooter, G., 2016. Spray drying formulation of amorphous solid dispersions. Adv. Drug Deliv. Rev Amorphous Pharmaceutical Solids 100, 27–50. https://doi.org/10.1016/j.addr.2015.12.010.
Sy, C., Gleize, B., Dangles, O., Landrier, J.-F., Veyrat, C.C., Borel, P., 2012. Effects of physicochemical properties of carotenoids on their bioaccessibility, intestinal cell uptake, and blood and tissue concentrations. Mol. Nutr. Food Res. 56, 1385–1397. https://doi.org/10.1002/mnfr.201200041.
Taylor, L.S., Zhang, G.G.Z., 2016. Physical chemistry of supersaturated solutions and implications for oral absorption. Adv. Drug Deliv. Rev. 101, 122–142. https://doi.org/10.1016/j.addr.2016.03.006.
Ting, J.M., Porter, W.W.I., Mecca, J.M., Bates, F.S., Reineke, T.M., 2018. Advances in polymer design for enhancing oral drug solubility and delivery. Bioconjug. Chem. 29, 939–952. https://doi.org/10.1021/acs.bioconjchem.7b00646.
Trumpower, B., 2012. Function of quinones in energy conserving systems. Elsevier.
Trzeciak, K., Chotera-Ouda, A., Bak-Sypien, I.I., Potrzebowski, M.J., 2021. Mesoporous silica particles as drug delivery systems—the state of the art in loading methods and the recent Progress in analytical techniques for monitoring these processes. Pharmaceutics 13, 950. https://doi.org/10.3390/pharmaceutics13070950.

Vraníková, B., Niederquell, A., Šklubalová, Z., Kuentz, M., 2020. Relevance of the theoretical critical pore radius in mesoporous silica for fast crystallizing drugs. Int. J. Pharm. 591, 120019 https://doi.org/10.1016/j.ijpharm.2020.120019.

Waters, L.J., Hanrahan, J.P., Tobin, J.M., Finch, C.V., Parkes, G.M.B., Ahmad, S.A., Mohammad, F., Saleem, M., 2018. Enhancing the dissolution of phenylbutazone using syloid® based mesoporous silicas for oral equine applications. J. Pharm. Anal. 8, 181–186. https://doi.org/10.1016/j.jpha.2018.01.004.

Wolbert, F., Nikoleit, K., Steinbrink, M., Luebbert, C., Sadowski, G., 2022. The shelf life of ASDs: 1. measuring the crystallization kinetics at humid conditions. Mol. Pharm. 19, 2483–2494. https://doi.org/10.1021/acs.molpharmaceut.2c00188.